Zero delay synchronization of chaos in coupled map lattices

M. S. Santhanam and Siddharth Arora
Physical Research Laboratory, Navrangpura, Ahmedabad 380 009, India
(Received 11 December 2006; revised manuscript received 10 May 2007; published 3 August 2007)

We show that two coupled map lattices that are mutually coupled to one another with a delay can display zero delay synchronization if they are driven by a third coupled map lattice. We analytically estimate the parametric regimes that lead to synchronization and show that the presence of mutual delays enhances synchronization to some extent. The zero delay or isochronal synchronization is reasonably robust against mismatches in the internal parameters of the coupled map lattices, and we analytically estimate the synchronization error bounds.

DOI: 10.1103/PhysRevE.76.026202 PACS number(s): 05.45.Xt, 05.45.Ra, 05.45.Jn

I. INTRODUCTION

Synchronization is one possible form of emergent dynamics displayed by coupled oscillator systems, and this is seen in a wide variety of physical phenomena; e.g., synchrony among neural activity in the brain [1] and intensity of coupled lasers to light pulses emitted by fireflies [2]. It is now well established that two chaotic systems, with appropriate coupling, can exhibit synchronized behavior [3,4]. Synchronized chaotic dynamics has been reported in systems consisting of well-known models of chaos like the logistic map, Lorentz system, Henon map, coupled map lattices, etc., which represent a wide collection of discrete and continuous time systems. The growing interest in chaos and synchronization is partly due to its potential applications in chaos control, chaos-based cryptography, neural networks, and biological systems.

Much of the work on synchronization has concentrated on instantaneous coupling of the dynamical systems [2]. This implies that we disregard the finite time it takes for the interaction or the information to travel from one system to the other. Consider two identical chaotic systems represented by $x_{n+1}=F(x_n)$ and $y_{n+1}=F(y_n)$, started from different initial conditions. To synchronize their solutions x_n and y_n, we suitably couple both the systems. Then the modified equations will be $x_{n+1}=F(x_n)+g_1(y_n)$ and $y_{n+1}=F(y_n)+g_2(x_n)$. In this form of coupling, we have implicitly assumed that y_n is instantly available to the x-system without any delay and vice versa. This cannot be true in general. Many physical phenomena that display synchronization are often spatially separated, and the time taken for the information to travel is not negligible. For example, synchronization of neuronal activity in the brain involves time delays due to information processing and transfer between different parts of the brain [5] and is estimated to be about tens of milliseconds [6]. In the context of using chaos synchronization for secure communication, it is usual for the sender and receiver to be spatially separated and information takes a finite time to travel between them. Then, the question is, can the delayed interactions lead to synchronization of coupled systems? The works done in the last few years show that delayed couplings can lead to synchronization [7,8] as well as new scenarios such as amplitude death in limit cycle oscillators and coupled oscillators [9], multistable synchronization [10], and symmetry breaking [11]. Techniques for controlling pathological rhythms in neurons based on delayed feedback have also been reported [12].

The experiments on information processing in the brain and neurosciences are providing evidence for new features of delayed synchronization: namely, that of near zero delay synchronization of signals from spatially separated regions [13]. It has been reported that spatially separated cortical regions in the brain of the cat display synchronization *without any lag* [14]. Neuronal firings from left and right cortex regions recorded on primates show near-zero synchrony maintained over considerable distances [15]. The idea of spatially distributed systems synchronizing without delay continues to attract research attention since the mechanism leading to such an effect is not yet clear and continues to be debated [16].

Recently one mechanism for zero delay synchronization of mutually coupled oscillators has been demonstrated experimentally in a system of three semiconductor lasers [17]. In this case, a central driving laser L_2 is bidirectionally coupled with two other mutually delay coupled lasers L_1 and L_3. Then, the delay coupled lasers L_1 and L_3 display zero delay or isochronal synchronization and are shown to be reasonably robust. A variant of this scheme has been used to propose a method for bidirectional secure communication using delay coupled oscillators [18]. Simultaneously, the modeling and analysis of zero lag synchronization maintained over large distances in neurons is beginning to take shape [19].

In this paper, we show that zero delay synchronization can be achieved in delay-coupled spatially extended systems—namely, a coupled map lattice (CML)—if they are driven by a third such system. This application is motivated by the fact that the activity in the cerebral cortex of the brain [as measured by an electroencephalograph (EEG), for example] is due to the interaction between millions of neurons that are spatially distributed. Zero lag synchronization occurs between groups of such spatially distributed neurons. Hence one is led to consider a collection of coupled oscillators that are spatially separated. Another important application is in the area of secure communication. Coupled map lattices can be applied to encryption of messages in multichannel communication [20]. In real time, for multichannel communications that require security, there is a need for as many different chaotic signals as the number of channels to encode the

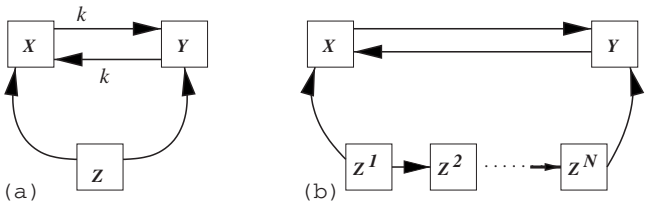

FIG. 1. Coupling scheme of CMLs. (a) x and y are mutually delay coupled CMLs. The z CML is the driver. (b) The driver is a collection of N unidirectionally coupled CMLs. k denotes the delay time in mutual coupling.

messages sent in each of the channels. Signals in these channels are encoded by the chaotic time series from one of the lattice points of the CML. The CML, being a high-dimensional chaotic system, provides sufficient security against most attacks. The presence of chaotic, zero delay synchronization would allow the receiver to decode the message in all channels at the same time. For real-time applications synchronization must be achieved in the shortest possible time and zero delay synchronization is ideally suited for this purpose. For a review of certain aspects of synchronization in spatially extended systems and its applications, see Ref. [21].

In the next section, we briefly review the coupled map lattice paradigm and introduce our model. Further, in subsequent sections, we report results on zero lag synchronization from this model and obtain analytically the parametric regimes where this occurs and also bounds for synchronization errors due to parameter mismatches.

II. COUPLED MAP LATTICE

We consider the coupled map lattice given by

$$x_{n+1}^i = (1-\epsilon) f[x_n^i] + \frac{\epsilon}{2}(f[x_n^{i-1}] + f[x_n^{i+1}]), \tag{1}$$

where $i=1,2,\ldots,L$ is the index for the lattice site and ϵ is the coupling strength parameter. This was originally introduced [22,23] as a model for chaos in spatially extended systems. There have been attempts to model real-life phenomena based on CMLs [23]. They display a rich variety of dynamical regimes ranging from frozen random patterns to spatiotemporal chaos upon variation of the parameters. We use periodic boundary conditions, so that $x_n^{L+1}=x_n^1$, leading to a ring-type lattice. Here, the local dynamics uses the logistic equation $f[x]=ax(1-x)$, where a is the chaos parameter. In Sec. V, we will denote this map showing its explicit parameter dependence as $f[x,a]$.

In this work, we are attempting to synchronize two CMLs labeled x and y at zero delay when both are mutually delay-coupled and are driven by a third CML labeled z. This is schematically shown in Fig. 1(a). The second CML labeled y is obtained by replacing x with y in Eq. (1); CML z can be obtained in a similar way. We mutually couple x and y CMLs with a delay. The z CML is the driver, and it is unidirectionally coupled to x and y CMLs. It is given by

$$z_{n+1}^i = (1-\epsilon) f[z_n^i] + \frac{\epsilon}{2}(f[z_n^{i-1}] + f[z_n^{i+1}]). \tag{2}$$

The modified form of the x CML is given by

$$x_{n+1}^i = \Gamma\{f[x_n^i] + \beta f[y_{n-k}^i] + \alpha f[z_n^i]\} + \frac{\epsilon}{2}\{f[x_n^{i-1}] + f[x_n^{i+1}]\}, \tag{3}$$

where $\Gamma=(1-\epsilon)/(1+\alpha+\beta)$. Similarly, the y CML is also modified and becomes

$$y_{n+1}^i = \Gamma\{f[y_n^i] + \beta f[x_{n-k}^i] + \alpha f[z_n^i]\} + \frac{\epsilon}{2}\{f[y_n^{i-1}] + f[y_n^{i+1}]\}. \tag{4}$$

Equations (2)–(4) represent our coupling scheme shown in Fig. 1(a) for zero lag synchronization. The parameters $\beta \geq 0$ and $\alpha \geq 0$ represent the strength of delayed mutual coupling and the strength of coupling with the driver CML, respectively. Note that in Eqs. (3) and (4), delay k is introduced in the mutual coupling term. If $\alpha=0$ (absence of a drive CML), then no isochronal synchronization takes place between $x_n(i)$ and $y_n(i)$ in the presence of mutual delays between them. However, if $\beta=0$, these CMLs synchronize beyond some critical value of α. We will explore the general case when $\alpha,\beta \geq 0$, $k>0$ and show numerical evidence for zero lag synchronization of x and y CMLs but not with the z CML. The coupling parameters ϵ and a are chosen such that the CML generates chaotic motion.

The coupling scheme shown in Fig. 1(a) is reminiscent of the generalized synchronization (GS) that has been widely studied in the last one decade [26]. In the GS scenario, there is one driver and a driven (response) system and the state of the latter depends on the former. This is the likely case in the absence of mutual coupling—i.e., $\beta=0$. However, in this scheme we are considering one driver and two driven systems which themselves are mutually coupled to one another with a delay. It is also relevant to point out that in this scheme the driver and the driven system need not necessarily be one unit each, but can be composed of many (sub)systems as shown in Fig. 1(b). In this scheme, instead of one driver CML, a collection of N unidirectionally coupled CMLs are used to drive the x and y CMLs. Detailed results for this scheme will be presented elsewhere.

III. ZERO DELAY SYNCHRONIZATION

The coupled map lattices in Eqs. (2)–(4) with $L=1000$ lattice elements are iterated for 6000 discrete time steps. Each of the CMLs is initialized at $n=0$ with a different realization of uniformly distributed random numbers. The logistic map parameter is $a=4.0$ such that the local map dynamics is chaotic and the local coupling strength is $\epsilon=0.1$. For this combination of a and ϵ, the CML in Eq. (1) is known to display spatiotemporal chaos [23]. The x and y CMLs are mutually coupled with a delay of $k=26$. The z CML drives both the x and y CMLs. In Fig. 2, we show a typical time series for x_n, y_n, and z_n drawn from the 525th lattice point

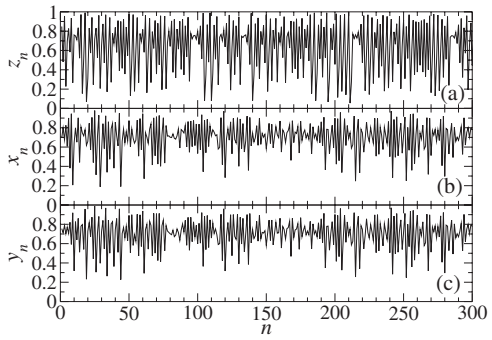

FIG. 2. (a) z_n, (b) x_n, and (c) y_n for the 525th lattice site of the CML system in Eqs. (2)–(4). The local map parameter is $a=4.0$. The local coupling strength in CMLs is $\epsilon=0.1$ and $\alpha=\beta=1.0$. The x and y CMLs are mutually coupled with delay $k=26$.

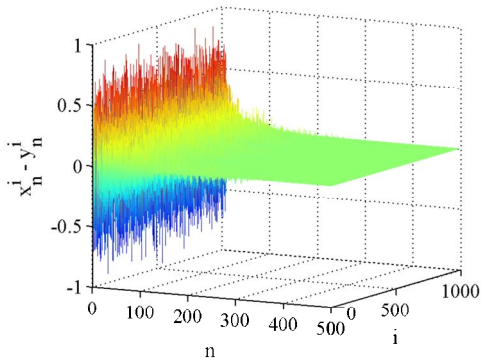

FIG. 4. (Color online) The quantity $x_n^i - y_n^i$ plotted as function of i and n. Notice that the region beyond $n>100$ is flat, indicating synchronization without delay in the entire coupled map lattice. The parameters are the same as in Fig. 2.

from the system of CMLs given by Eqs. (2)–(4). Notice that each of them is chaotic, and beyond the 100th time step x_n and y_n are synchronized without delay. The difference between the pairs of time series is shown in Fig. 3, and clearly the delay-coupled CMLs x and y exhibit isochronal synchronization [Fig. 3(c)], but they do not synchronize with the driver z CML as seen in Figs. 3(a) and 3(b). Even though the results from a typical time series from one lattice point are displayed in Figs. 2 and 3, we observe synchronization for all the lattice points of x and y coupled map lattices. This is shown in Fig. 4 as a space-time plot which has a flat region coinciding with zero of the z axis for $n>100$ at every lattice point.

The isochronal synchronization of CMLs demonstrated in Fig. 4 depends on the strength parameters α and β. Results presented here indicate that there is a critical value of α and β, other parameters remaining the same, below which synchronization does not take place. However, the time taken to achieve synchrony is found to increase with the magnitude of the delay k. The effect of various parameters on synchronization is discussed in the next section. In order to understand the correlations that exist between x_n, y_n, and z_n at the ith lattice site, we study the lagged cross correlation defined as

$$C(m) = \frac{\sum_{n=1} (x_n - \bar{x})(y_{n+m} - \bar{y})}{\sigma_x \sigma_y}, \tag{5}$$

where $\bar{x}$ and $\bar{y}$ are the sample means, σ is the corresponding standard deviation, and m represents the lag; the lattice site index is suppressed. In Fig. 5, the solid line shows the lagged cross correlation between the iterates of x and y CMLs at the 525th lattice site. At zero lag, x_n and y_n are almost perfectly correlated with $|C(0)|=0.998$, indicating perfect synchronization without delay. Along with this, the mutual coupling between x and y CMLs with delay $k=26$ leads to partial recurrences in $|C(m)|$ at similar intervals. In contrast, for x_n and z_n (dashed line in Fig. 5), $|C(0)|=0.701$ indicates the absence of identical synchronization [see also Figs. 3(a) and 3(b)]. Due to synchrony between x_n and y_n, again a similar result holds for y_n and z_n, with peaks in $|C(m)|$ separated by delay $k=26$. If we apply instantaneous coupling—i.e., $k=0$—then the recurrences would be absent, as shown by the dotted line in Fig. 5, indicating that x and y CMLs would not maintain any memory of the dynamics of the other CMLs in

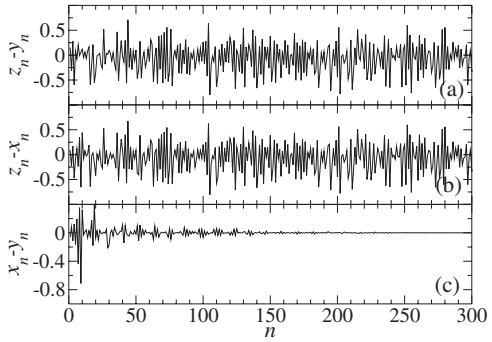

FIG. 3. (a) $z_n - y_n$, (b) $z_n - x_n$, and (c) $x_n - y_n$. The parameters are the same as in Fig. 2.

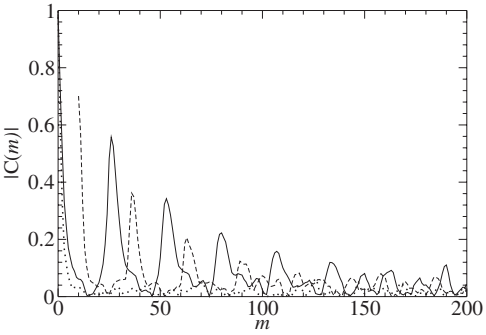

FIG. 5. Absolute cross correlation $|C(m)|$ as a function of lag m. $|C(m)|$ between x_n and y_n (solid line) and between x_n and z_n (dashed line) taken from their 525th lattice point is displayed. The dashed line is shifted by 10 units along the x axis for clarity. The cross correlation between y_n and z_n is almost indistinguishable from the dashed line since x_n and y_n are in synchrony. If mutual coupling is absent ($k=0$), then recurrences are not seen (dotted line).

them. Similar results hold for all lattice sites in CMLs.

The recurrence pattern of $|C(m)|$ shown in Fig. 5 can be used to detect mutually delayed couplings and estimate the magnitude of delay in real physical systems. As shown in that figure, the absence of delayed couplings would not lead to any recurrence. It is essential that the physical system should be composed of many subsystems which can display synchronization among themselves. The time interval between the peaks in $|C(m)|$ would give an estimate of the magnitude of delay. However, in a complex physical system, the cross correlations alone will not be sufficient in identifying the driver system. At this point, we also remark about the possibility of replacing a z CML by a noise process. Do we expect synchronization then? In some restricted range of parameters, the same noise process driving both x and y CMLs can lead to isochronal synchronization. However, the neat recurrence structures and the associated memory features shown in Fig. 5 will be absent in such a case and the magnitude of delays will not carry any significance.

IV. SENSITIVITY TO PARAMETERS

In this section, we discuss the parametric regimes in which the synchronization occurs. As pointed out before, isochronal synchronization depends on the parameters k, α, and β. To understand the role of these parameters, we apply linear stability analysis. The synchronized solution of interest is

$$u_{n+1}^i = x_{n+1}^i - y_{n+1}^i = \bar{u}_{n+1} \quad \text{for all } n. \tag{6}$$

In our case, $\bar{u}_{n+1}=0$. We will perform a linear stability analysis of this solution to determine the parameters that will lead to synchronization. For convenience, we will shift to new variables defined as

$$u_n^i = x_n^i - y_n^i, \quad v_n^i = x_n^i + y_n^i. \tag{7}$$

The dynamics of u_{n+1}^i can be written as

$$u_{n+1}^i = \frac{g(u_n^i, v_n^i)}{1+\alpha+\beta} - \frac{\beta(1-\epsilon)}{1+\alpha+\beta} g(u_{n-k}^i, v_{n-k}^i) + \epsilon \left\{ \sum_{j\sim i} g(u_n^j, v_n^j) - \frac{g(u_n^i, v_n^i)}{1+\alpha+\beta} \right\}, \tag{8}$$

where $g(u_n^i, v_n^i) = f(x_n^i) - f(y_n^i) = a u_n^i (1 - v_n^i)$ and $j \sim i$ represents summation over nearest neighbors. We will follow the elegant technique discussed in Ref. [24]. The connection topology, here being the nearest neighbor, is encoded in the spectra of the graph Laplacian defined as $(\Delta w)_i = (1/n_i)\Sigma_{j\sim i}(w_j - w_i)$. We will use the fact that the eigenmodes ϕ of the Laplacian are obtained from the eigenvalue equation $\Delta\phi_m = -\lambda_m \phi_m$ [24], where $-\lambda_m$ is the eigenvalue. Then, we will consider perturbations to synchronized solution $\bar{u}_n$ in Eq. (6) by the mth eigenmode ϕ_m^i as

$$u_n^i = \bar{u}_n + \mu \delta u_n^m \phi_m^i, \tag{9}$$

such that for $\mu \ll 1$, $\delta u_m(n) \to 0$ as $n \to \infty$ for synchronized solutions. Substituting this in $g(u_n^i, v_n^i)$ and Taylor expanding it about $\mu = 0$, we get

$$g(u_n^i, v_n^i) = g(\bar{u}_n, v_n^i) + \mu \delta u_n^m \phi_m^i g'(\bar{u}_n), \tag{10}$$

and $g'(\bar{u}_n)$ should be taken to mean $g(u_n^i, v_n^i)$ evaluated at the synchronized solution $\bar{u}_n$. We substitute this into Eq. (8) to obtain

$$\delta u_{n+1}^m \phi_m^i = \left\{ \frac{\epsilon}{1+\alpha+\beta} \Delta\phi_m^i + \frac{1}{1+\alpha+\beta} \phi_m^i \right\} \delta u_n^m g'(\bar{u}_n) - \frac{\beta(1-\epsilon)}{1+\alpha+\beta} \delta u_{n-k}^m \phi_m^i g'(\bar{u}_{n-k}). \tag{11}$$

Using $\Delta\phi_m = -\lambda_m \phi_m$ and after some simple manipulations, we get

$$\delta u_{n+1}^m = \left(\frac{1-\lambda_m \epsilon}{1+\alpha+\beta} \right) \delta u_n^m g'(\bar{u}_n) - \frac{\beta(1-\epsilon)}{1+\alpha+\beta} \delta u_{n-k}^m g'(\bar{u}_{n-k}). \tag{12}$$

This is the relation we need to analyze the stability of synchronized solutions. The eigenvalue $-\lambda_m$ is dependent only on the connection topology of the CML. For nearest-neighbor coupling, the nonzero eigenvalues of Δ are $\lambda_m = 1 - \cos(2\pi m/L)$, $m = 1, 2, \ldots, L-1$ [24]. If $L \gg 1$, the largest eigenvalue is 2 if L is even and $1 + \cos(\pi/L) \sim 2$ if L is odd. Putting $\lambda_m = 2$, Eq. (12) can be analyzed for the following two cases.

A. Absence of mutual coupling, $\beta = 0$

First, we consider the case $\beta = 0$—i.e., the absence of mutual coupling. In this case, we have, from Eq. (12),

$$\delta u_{n+1}^m = \left(\frac{1-2\epsilon}{1+\alpha} \right) \delta u_n^m g'(\bar{u}_n). \tag{13}$$

The condition for local stability is

$$q = \lim_{N\to\infty} \frac{1}{N} \ln \frac{|\delta u_{N+1}^m|}{|\delta u_0^m|} < 0. \tag{14}$$

Since $g'(\bar{u}_n) = f'(x_n)$, we can iterate Eq. (13) N times to obtain

$$q = \ln \left| \frac{1-2\epsilon}{1+\alpha} \right| + \langle \ln |f'(x_n)| \rangle, \tag{15}$$

where $\langle \cdot \rangle$ denotes the time average. If the local map $f(x_n)$ is ergodic, this average can be replaced by an ensemble average and we have $\langle \ln |f'(x_n)| \rangle = \ln 2$, the Lyapunov exponent of the logistic map. Hence, the condition for synchronization for $\beta = 0$ turns out to be $|2(1-2\epsilon)/(1+\alpha)| < 1$, which implies

$$\alpha > |2 - 4\epsilon| - 1. \tag{16}$$

This holds good for any value of k, as is to be expected. Second, note that if $\alpha = 0$, the stability condition in Eq. (16) will not be satisfied for any value of ϵ for which synchronization takes place. Hence, for $\alpha = 0$—i.e., in the absence of a drive CML—no isochronal synchronization can take place. This condition is verified by numerical simulations of CMLs in Eqs. (2)–(4) with $\epsilon = 0.1$ and $\beta = 0$. We define the degree of synchronization to be

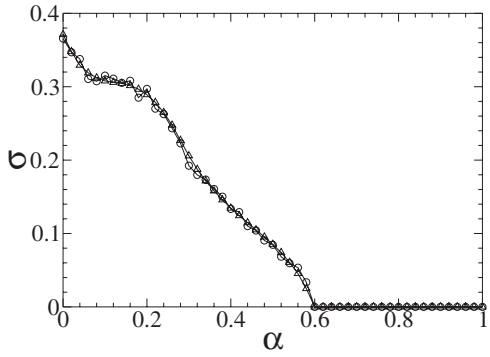

FIG. 6. Degree of synchronization, σ, as a function of α for $\beta=0$ and $\epsilon=0.1$. The delays are $k=4$ (circles) and $k=24$ (triangles).

$$\sigma = \langle (x_n^i - y_n^i)^2 \rangle, \tag{17}$$

where the average $\langle \cdot \rangle$ is taken over all the lattice points for 50 000 iterations after discarding the initial 10 000 time steps [8]. If the system synchronizes, then $\sigma \to 0$ as $n \to \infty$. The results in Fig. 6 show that for $\alpha > 0.6$, we obtain $\sigma < 10^{-20}$, leading to synchronization, and this confirms the validity of analytical condition in Eq. (16).

B. Effect of delays, $\beta > 0$

Next, we consider the case $\beta > 0$. In this case, it is not straightforward to analytically solve Eq. (12) to obtain local stability criteria. We iterate Eq. (12) numerically to estimate the value of q [Eq. (14)] as a function of α and β for $\epsilon = 0.1$. In Fig. 7, we present the numerical results, and if $q < 0$, we denote it by a black point (synchronization) and for $q > 0$ we denote it by white point (no synchronization). The interesting feature is that the introduction of delays enhances synchronization to some extent. For instance, at $\beta=0$, synchrony requires $\alpha > 0.6$, but in the presence of delays, approximately $\alpha > 0.4$ is sufficient for synchronization in the range $\sim 0.15 < \beta < 0.5$. This is reminiscent of recent results that indicate enhanced synchrony due to the presence of delays in coupled systems [7,8]. As the strength of mutual coupling β increases, it will require an even stronger drive by z CMLs to achieve synchronization. This can be qualitatively seen in Fig. 7 where for $\beta > 0.5$ the minimum value of α

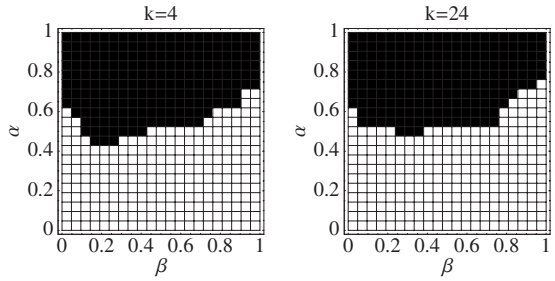

FIG. 7. Degree of synchronization, σ, as a function of α and β, obtained by numerically iterating Eq. (12). The results are shown for two different choices of delay k. The black points indicate $\sigma < 10^{-15}$, and white indicates a lack of synchronization.

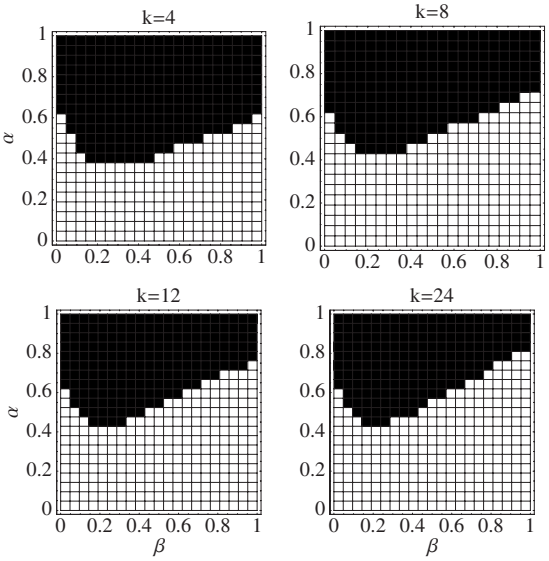

FIG. 8. Degree of synchronization σ, as a function of α and β, obtained by numerically simulating CMLs in Eqs. (2)–(4). The results are shown for four different choices of delay k. The black points indicate $\sigma < 10^{-15}$, and white indicates a lack of synchronization.

required for synchronization increases with an increase in β. Notice again that at $\alpha=0$ there is no synchronization, even in the presence of delays.

To confirm the linear stability analysis for $\beta > 0$, in particular the results displayed in Fig. 7, we simulate the CMLs in Eqs. (2)–(4) as a function of α, β, and k and we display the degree of synchronization, σ, in Fig. 8. The black points in the figure denote $\sigma < 10^{-15}$, and white points correspond to lack of synchronization. This is shown for four different choices of delays k. The CML simulations broadly agree with the numerical estimates of q shown in Fig. 7 based on Eq. (12). The features such as the enhancement in synchronization in the presence of delays and optimal β is clearly seen in these simulations. While a physical explanation for enhanced synchrony and the optimal value of β is not yet clear, one plausible reason could be as follows: For $\alpha=\beta=0$, we have two independent chaotic CMLs. But in the absence of only the driver CML—i.e., with $\alpha=0$—the dynamics of the CML system, $x_n(i)$ and $y_n(i)$, for $0.03 < \beta < 0.14$ settles mostly to a periodic solution and for $\beta > 0.14$ it becomes increasingly chaotic. Thus, in parametric space, there is a window of a nonchaotic region flanked on either side by predominantly chaotic dynamics. The strength of the driver α required to synchronize the nonchaotic dynamics is less than the one needed for a chaotic solution. This accounts for the dip around $\beta=0.1-0.2$ seen in Figs. 7 and 8.

Furthermore, it is only to be expected that as k increases synchrony would be difficult to achieve and hence strong driving by z CMLs will be needed to enforce synchronization. Thus, if β is held constant, the minimal α required to bring about synchronization increases as the mutual coupling delay k increases. At $k=\infty$, the delay is infinite and the x and y CMLs do not communicate with each other on finite time scales. This scenario corresponds to setting $\beta=0$, the absence

of mutual coupling. Indeed, if k is larger than the simulation times, we obtain similar results as shown in Fig. 6. Even though we use values of k in multiples of 4, we emphasize that the qualitative results remain unaltered for all even values of k. However, for odd values of k, the synchronization region in (α,β) space is smaller compared to those displayed in Fig. 8. A better analytical handle on solutions of Eq. (12) will help understand the role of odd k.

V. ROBUSTNESS

How robust is this zero delay synchronization against parameter mismatches? This question is of practical importance since in real-life systems, be it EEG signals in the brain or electronic circuits for encryption in communications, most often the parameters remain mismatched. For the purposes of this section, we will explicitly show the parameter dependence in the CMLs; for instance, the x CML in Eq. (3) will be denoted by $x^i_{n+1}(a,\epsilon)$ and the local map will be denoted by $f[x^i_n;a]$. We will consider the quantity, to be called synchronization error,

$$S^i_{n+1}(a_1,\epsilon_1;a_2,\epsilon_2) = x^i_{n+1}(a_1,\epsilon_1) - y^i_{n+1}(a_2,\epsilon_2). \quad (18)$$

The synchronization time T_{sync} is defined such that $S^i_{n+1}(a_1,\epsilon_1;a_2,\epsilon_2)=0$ for all $n>T_{sync}$. For most practical purposes, T_{sync} should be typically much smaller than the experimental times of interest. We will consider the synchronization error in Eq. (18) and analytically estimate the bounds on S^i_{n+1} due to parameter mismatches. In the case of identical synchronization without delay, we have shown above that $S^i_{n+1}=0$ for all i and for all $n>T_{sync}$.

First, we note that identical synchronization persists—i.e., $S_{n+1}(i)=0$ for reasonably large mismatches of the local map parameter a between the driver CML and the driven CMLs. In particular, the numerical simulations indicate that synchronization is mostly independent of the coupling constant ϵ in the z CML. Hence the important effects arise due to mismatch in parameters of the x- and y CMLs, which we study below. In the numerical simulations shown in this section, we have maintained $\alpha=\beta=1$ and $k=26$.

A. Mismatch in the local map parameter

We consider the effect of mismatch in the parameters of x and y CMLs. First, we consider the case when the parameters of the x and z CMLs are identical, but there is a mismatch Δa in the local map parameter between x and y CMLs. Starting from Eqs. (3) and (4), after some algebra, we obtain S^i_{n+1} without any approximation as

$$S^i_{n+1}(a,\epsilon;a-\Delta a,\epsilon) = S^i_{n+1}(a,\epsilon;a,\epsilon) + \phi_1(\Delta a,\epsilon), \quad (19)$$

where we have

$$\phi_1(\Delta a,\epsilon) = \Gamma(f[y^i_n;\Delta a] - \beta f[y^i_{n-k};\Delta a]) + \frac{\epsilon}{2}(f[y^{i-1}_n;\Delta a] + f[y^{i+1}_n;\Delta a]). \quad (20)$$

For $n>T_{sync}$, we will have $S^i_{n+1}(a,\epsilon;a,\epsilon)=0$, which is the condition for zero lag synchronization and has been numerically demonstrated in the previous section. Notice that for the logistic map, $0\le f[x_n;a]=a\ g(x_{n-1})\le 1$, where $g(x)=x(1-x)$. Hence the first term in Eq. (20) is smaller compared to the second term and we have the approximate result that

$$S^i_{n+1}(a,\epsilon;a-\Delta a,\epsilon) \approx \frac{\epsilon\Delta a}{2}(g[y^{i-1}_n] + g[y^{i+1}_n]) \le \frac{\epsilon\Delta a}{2} g_{\max} \approx \frac{\epsilon\Delta a}{2}, \quad (21)$$

where $g_{\max}=\max(g[y^{i-1}_n]+g[y^{i+1}_n]) \sim O(1)$. Thus, in the case of mismatch in the parameter a, the upper bound for synchronization error is of $O(\epsilon\Delta a/2)$. This estimate can be compared with the average synchronization error after evolving it for a sufficiently long time as shown in Figs. 9(a) and 9(c). The root-mean-square deviation or the standard deviation $\sigma_S(\Delta a)$ of $S^i_{n+1}(a,\epsilon;a-\Delta a,\epsilon)$ is a suitable measure and is obtained by numerically simulating Eqs. (2)–(4). In Fig. 9(b), we show $\langle\sigma_S(\Delta a)\rangle$, the averaged standard deviation over all lattice sites, and we observe good agreement with the analytical results.

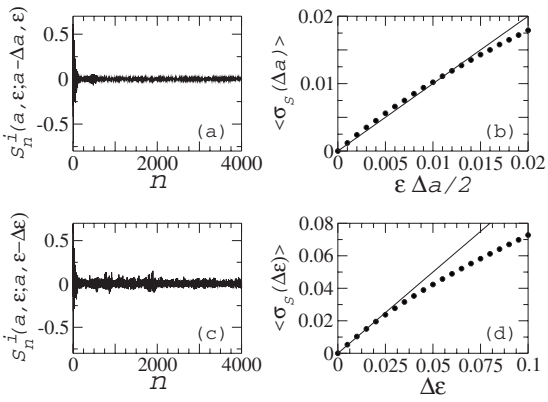

FIG. 9. (a) S^i_n for the $i=525$th lattice with $a=4.0$, $\epsilon=0.1$, and $\Delta a=0.1$. (b) $\langle\sigma_S(\Delta a)\rangle$, the standard deviation of S^i_n averaged over all lattice sites, as a function of Δa. (c) S^i_n for the $i=525$th lattice with $a=4.0$, $\epsilon=0.1$, and $\Delta\epsilon=0.05$. (d) $\langle\sigma_S(\Delta\epsilon)\rangle$ as a function of $\Delta\epsilon$. Note that the synchronization error due to parameter mismatch is bounded by estimates in Eqs. (21) and (24) shown as solid lines in (b) and (d).

B. Mismatch in the coupling constant

We consider the case when all the three CMLs in Eqs. (2)–(4) have the same chaos parameter a, but the local coupling strength in the x and z CMLs is ϵ and for the y CML it is $\epsilon+\Delta\epsilon$. Typically, $\Delta\epsilon\ll 1$. Once again, we start from Eqs. (3) and (4) and we obtain

$$S^i_{n+1}(a,\epsilon;a,\epsilon-\Delta\epsilon) = S^i_{n+1}(a,\epsilon;a,\epsilon) + \Delta\epsilon\phi_2, \quad (22)$$

$$\phi_2 = -\tfrac{1}{3}(f[y^i_n;a] + \beta f[x^i_{n-k};a] + \alpha f[z^i_n;a]) + \tfrac{1}{2}(f[y^{i-1}_n;a] + f[y^{i+1}_n;a]). \quad (23)$$

As before, $S^i_{n+1}(a,\epsilon;a,\epsilon)=0$ in Eq. (22) which defines the synchronization state. For the logistic map $0\leq f(x;a)\leq 1$, and hence we have $|\phi_2|\leq 1$. Thus, if the coupling parameters are mismatched, the synchronization is still present, though it suffers an error whose bound is estimated to be

$$S^i_{n+1}(a,\epsilon;a,\epsilon-\Delta\epsilon)\leq \Delta\epsilon. \tag{24}$$

Figure 9(d) shows that the numerically simulated synchronization error, quantified by the average standard deviation $\langle\sigma_S(\Delta\epsilon)\rangle$ of $S^i_{n+1}(a,\epsilon;a,\epsilon-\Delta\epsilon)$ over all lattice sites, is always lesser than the analytical bound which is linear in $\Delta\epsilon$.

It must be remarked that in both cases of parameter mismatches studied above synchronization suffers an error that can be minimized by tuning Δa or $\Delta\epsilon$. In other words, for large mismatches $(\Delta a,\Delta\epsilon\gg 1)$ synchronization is completely lost as seen from the trends in numerical results in Figs. 9(b) and 9(d). Obviously, exactly identical synchronization without lag is recovered if the mismatches Δa and $\Delta\epsilon$ are zero. It is possible that there can be mismatches in both a and ϵ. Proceeding as above, we can obtain an estimate for the error bounds as

$$S^i_{n+1}(a,\epsilon;a-\Delta a,\epsilon-\Delta\epsilon)=S^i_{n+1}(a,\epsilon;a,\epsilon)+\chi_1\Delta a + \chi_2\Delta\epsilon+\chi_3\Delta a\Delta\epsilon, \tag{25}$$

where $\chi_1,\chi_2,\chi_3\leq 1$. Once synchronization is reached, $S^i_{n+1}(a,\epsilon;a,\epsilon)=0$. Thus, depending on the relative magnitude of Δa, $\Delta\epsilon$, and $\Delta a\,\Delta\epsilon$, the dominant synchronization error bound has a linear dependence on one of these factors. In fact, the error analysis done above would hold good for any local map of the form $f[x;a]=a\,g(x)$. Experiments in neuronal studies have reported examples of synchronization with an error in spatially distributed neurons [25]. From the form of the analytical estimates in Eqs. (19), (21), and (24), it might appear as though the z CML has no role to play in synchronizing the coupled dynamics. The contribution of the z CML enters the x and y CMLs through the mutual coupling terms with the delay k.

VI. CONCLUSIONS

We have shown through numerical simulations that two coupled map lattices—say, x and y CMLs—which are coupled to one another with a delay can display *isochronal* synchronization if they are driven by a third CML. We have used periodic boundary conditions—i.e., a ring-type lattice—for the CMLs in the results presented here. The central result remains unaltered even if we use a different boundary condition; e.g., the one-way coupled map lattice with ring- or open-type boundary conditions. While isochronal synchronization is achieved irrespective of the boundary conditions, the parametric regimes in which this synchrony occurs depend on the boundary conditions. Our results also indicate that there is a critical value for the coupling strength ϵ above which the synchronization occurs. We have analytically studied how the strength parameters α and β and the delay k affect isochronal synchronization. An interesting feature is that the presence of delays leads to synchronization in a larger parametric regime when compared with the case of the absence of mutual coupling.

The original motivation for this work was to look for possible mechanisms that could explain isochronal synchronization occurring in neuronal systems [13]. For simplicity, we considered one-dimensional coupled map lattices with nearest-neighbor coupling even though they are not known to be models for a collection of neurons in the brain. However, we expect qualitatively similar results for models of neurons, too [27]. In general, higher-dimensional extensions of CMLs are possible and they display a much richer variety of collective properties like phase-synchronized states and cluster synchronization [28] which could modify the scenario presented in this work. It would be interesting to study isochronal synchronization in higher-dimensional coupled map systems.

It is known that two mutually coupled oscillators synchronize with one another. However, the question of isochronal synchronization in mutually delay-coupled oscillators is currently being actively pursued in view of its applications in biological systems. The results discussed here provide one possible mechanism for isochronal synchronization in delay-coupled spatially extended systems. We have also obtained analytical estimates for bounds on errors due to mismatches in parameters between the two CMLs and verified them in simulations. We have also simulated this scheme with a one-way coupled map lattice [29], and qualitatively the results are the same as discussed above. It would be interesting to study isochronal synchronization in delay-coupled physical systems and in their realistic models. Further, other coupling topologies can also be implemented to study if synchronized solutions such as the one discussed here are supported in them. The results discussed in this work will help understand the effects of delay coupling in spatially separated, extended physical systems.

ACKNOWLEDGMENTS

One of us (S.A.) thanks the Physical Research Laboratory for an internship during which time part of this work was begun. We also thank the anonymous referee for critical comments that helped improve the manuscript.

[1] L. Glass, Nature (London) **410**, 277 (2001); R. Quian Quiroga, A. Kraskov, T. Kreuz, and P. Grassberger, Phys. Rev. E **65**, 041903 (2002).

[2] A. Pikovsky, M. Rosenblum, and J. Kurths, *Synchronization: A Universal Concept in Nonlinear Sciences* (Cambridge University Press, Cambridge, UK, 2001).

[3] H. Fujisaka and T. Yamada, Prog. Theor. Phys. **75**, 1087 (1986); L. M. Pecora and T. L. Carroll, Phys. Rev. Lett. **64**, 821 (1990).

[4] S. Boccaletti, J. Kurths, G. Osipov, D. L. Valladares, and C. S.

Zhou, Phys. Rep. **366**, 1 (2002).
[5] A. K. Engel, P. Knig, A. K. Kreiter, and W. Singer, Science **252**, 1177 (1991).
[6] H. Swadlow, in *Time and the Brain: Conceptual Advances in Brain Research*, edited by R. Miller (Harwood Academic, Amsterdam, 2000).
[7] C. Masoller and A. C. Marti, Phys. Rev. Lett. **94**, 134102 (2005); Yu. Jiang, Phys. Lett. A **267**, 342 (2000); C. Li *et al.*, Physica A **335**, 365 (2004); M. Dhamala, K. Victor Jirsa, and Mingzhou Ding, Phys. Rev. Lett. **92**, 074104 (2004).
[8] F. M. Atay, J. Jost, and A. Wende, Phys. Rev. Lett. **92**, 144101 (2004).
[9] D. V. Ramana Reddy, A. Sen, and G. L. Johnston, Phys. Rev. Lett. **80**, 5109 (1998); A. Prasad, Phys. Rev. E **72**, 056204 (2005).
[10] S. Kim, S. H. Park, and C. S. Ryu, Phys. Rev. Lett. **79**, 2911 (1997); U. Ernst, K. Pawelzik, and T. Geisel, Phys. Rev. E **57**, 2150 (1998).
[11] T. Heil, I. Fischer, W. Elsässer, J. Mulet, and C. R. Mirasso, Phys. Rev. Lett. **86**, 795 (2001).
[12] M. Rosenblum and A. Pikovsky, Phys. Rev. E **70**, 041904 (2004).
[13] J. Sarnthein *et al.*, Proc. Natl. Acad. Sci. U.S.A. **95**, 7092 (1998); S. F. Farmer, J. Physiol. **509**(1), 3 (1998).
[14] P. R. Roelfsema *et al.*, Nature (London) **385**, 157 (1997); C. M. Gray *et al.*, *ibid.* **338**, 334 (1989).
[15] V. N. Murthy and E. E. Fetz, J. Neurophysiol. **76**, 3968 (1996).
[16] W. J. Freeman, Int. J. Bifurcation Chaos Appl. Sci. Eng. **10**, 2307 (2000).
[17] I. Fischer, R. Vicente, J. M. Buldú, M. Peil, C. R. Mirasso, M. C. Torrent, and J. García-Ojalvo, Phys. Rev. Lett. **97**, 123902 (2006).
[18] R. Vicente, C. R. Mirasso, and Ingo Fischer, Opt. Lett. **32**, 403 (2007).
[19] A. Knoblauch and F. T. Sommer, Neurocomputing **58–60**, 185 (2004); T. Kanamaru, Neural Comput. **18**, 1111 (2006).
[20] J. H. Xiao, G. Hu, and Z. Qu, Phys. Rev. Lett. **77**, 4162 (1996); G. Hu, J. Xiao, J. Yang, F. Xie, and Z. Qu, Phys. Rev. E **56**, 2738 (1997); X. Wang *et al.*, Chaos **15**, 023109 (2005).
[21] S. C. Manrubia, A. S. Mikhailov, and D. H. Zanette, *Emergence of Dynamical Order: Synchronization Phenomena in Complex Systems* (World Scientific, Singapore, 2004).
[22] K. Kaneko, Prog. Theor. Phys. **72**, 480 (1984); I. Waller and R. Kapral, Phys. Rev. A **30**, 2047 (1984); K. Kaneko, Physica D **37**, 60 (1989).
[23] Chaos **2**(3) (1992), focus issue on coupled map lattices, edited by K. Kaneko; *Theory and Applications of Coupled Map Lattices*, edited by K. Kaneko (Wiley, New York, 1993).
[24] J. Jost and M. P. Joy, Phys. Rev. E **65**, 016201 (2001); F. M. Atay and Ö. Karabacak, SIAM J. Appl. Dyn. Syst. **5**, 508 (2006).
[25] P. Koenig *et al.*, Neural Comput. **7**, 469 (1995).
[26] N. F. Rulkov, M. M. Sushchik, L. S. Tsimring, and H. D. I. Abarbanel, Phys. Rev. E **51**, 980 (1995); H. D. I. Abarbanel, N. F. Rulkov, and M. M. Sushchik, *ibid.* **53**, 4528 (1996).
[27] Alexandra S. Landsman and Ira B. Schwartz (unpublished).
[28] H. Chaté and P. Manneville, Prog. Theor. Phys. **87**, 1 (1992); B. Hu and Z. Liu, Phys. Rev. E **62**, 2114 (2000); I. Belykh *et al.*, Chaos **13**, 165 (2003); K. Kaneko, Physica D **37**, 60 (1989).
[29] F. H. Willeboordse and K. Kaneko, Phys. Rev. Lett. **73**, 533 (1994).